ANSCOMBE MEETS HOUGH: NOISE VARIANCE STABLIZATION VIA PARAMETRIC MODEL ESTIMATION

Mariano Tepper, Andrea Giovannucci, and Eftychios Pnevmatikakis

Flatiron Institute, Simons Foundation, USA

ABSTRACT

In this work we pose the parameter estimation of the Poisson-Gaussian noise model as a parametric model estimation problem. We first take patches from the image/video to analyze and treat variance stabilization transforms, e.g., the classical Generalized Anscombe transform, as a parametric model, which we fit to the patches using the Hough transform. This algorithm allows to successfully estimate the noise parameters, is computationally efficient, and is fully parallelizable. We present an application to calcium imaging data, where the estimated parameters are used to enhance state-of-the-art processing pipelines.

Index Terms— Poisson-Gaussian noise, Generalized Anscombe transform, Hough transform, calcium imaging

1. INTRODUCTION

A common noise model in typical digital imaging chains is the Poisson-Gaussian [1, 2]. Under this model, an image $\mathbf{v}$ obtained with some digital image sensor is modeled as

$$\mathbf{v}(\mathbf{x}) = \alpha \mathbf{p}(\mathbf{x}) + \mathbf{n}(\mathbf{x}), \tag{1}$$

where $\mathbf{p}(\mathbf{x}) \sim \mathcal{P}(\mathbf{u}(\mathbf{x}))$ is the number of detected photons, $\mathbf{u}(\mathbf{x})$ is the noise-free and unknown image, $\alpha > 0$ is a constant scaling term (which depends on the sensor's efficiency and analog gain), and $\mathbf{n}(\mathbf{x}) \sim \mathcal{N}(\mu, \sigma^2)$ is signal-independent electric and thermal noise. The Poisson-Gaussian noise model is fully characterized by the parameters α, μ, and σ. Its first and second moments are

$$\mathrm{E}[\mathbf{v} \,|\, \mathbf{u}] = \alpha \mathbf{u} + \mu, \tag{2a}$$

$$\mathrm{var}[\mathbf{v} \,|\, \mathbf{u}] = \alpha^2 \mathbf{u} + \sigma^2. \tag{2b}$$

The vast majority of algorithms [3, 4, 5] for processing $\mathbf{v}$ assume, for simplicity, that it is only contaminated with Gaussian noise (i.e., $\mathbf{v} = \mathbf{u} + \mathbf{n}$). Variance stabilization seeks to eliminate the dependency between the noise-free image and the noise variance, Eq. (2b), allowing the use of the vast collection of off-the-shelf image processing algorithms [5]. This is usually done by applying a variance stabilization transform (VST), i.e., a function $f : \mathbb{R} \to \mathbb{R}$ such that

$$\mathrm{var}[f_{\alpha,\mu,\sigma}(\mathbf{v}) \,|\, \mathbf{u}] \approx 1. \tag{3}$$

A popular choice for such a function is the Generalized Anscombe transform (GAT) [6, 1],

$$f_{\alpha,\mu,\sigma}(\mathbf{z}) = 2\sqrt{\max\left(\tfrac{\mathbf{z}}{\alpha} + \tfrac{3}{8} + \tfrac{\sigma^2 - \alpha\mu}{\alpha^2}, 0\right)}. \tag{4}$$

Evidently, correctly estimating the parameters α, μ, σ is critical for proper variance stabilization. Notice that even algorithms that consider Poisson-Gaussian noise require a correct estimation of these parameters [5, 7].

In this paper, we show that the Poisson-Gaussian noise mode parameters can be found in a simple and yet efficient way. We first take patches from the image/video to analyze and treat the GAT as a parametric model, which we fit to the patches using the Hough transform (HT) [8]. The key insights behind this idea are two-fold. First, we often do not need a very high numerical precision in the estimated values. Second, although non-convex, the problem is very low-dimensional (just three scalars, but can be reduced to two without loss of generality).

The HT is a feature extraction technique used in image analysis, computer vision, and digital image processing [8]. The technique is used to find imperfect instances of objects within a certain class of shapes by a voting procedure. Our target shape is the zeroth iso-level of $\mathrm{var}[f_{\alpha,\mu,\sigma}(\mathbf{v}) \,|\, \mathbf{u}] - 1$.

The remainder of this paper is organized as follows. Sec. 2 describes the proposed method. In Sec. 3 we present an application to the analysis calcium imaging data, showing that correctly estimating the noise parameters enhances the performance of state-of-the-art processing pipelines. Finally, in Sec. 4 we offer some concluding remarks.

2. ESTIMATING POISSON-GAUSSIAN NOISE WITH THE HOUGH TRANSFORM

The rationale behind the GAT, Eq. (4), is quite simple. Using the first-order Taylor expansion of a VST f around $\mathbf{z} = \alpha\mathbf{u} + \mu$, we can approximate

$$\begin{aligned}\mathrm{var}[f(\mathbf{v}) \,|\, \mathbf{u}] &\approx \mathrm{var}[f(\mathbf{z}) + f'(\mathbf{z})\,(\mathbf{v} - \mathbf{z}) \,|\, \mathbf{u}] \\ &\approx \left(f'(\mathbf{z})\right)^2 \mathrm{var}[\mathbf{v} \,|\, \mathbf{u}].\end{aligned} \tag{5}$$

Using Eq. (3) and assuming that the approximations hold exactly, we can pose $f'(\mathbf{z}) = (\alpha^2\mathbf{u} + \sigma^2)^{-1/2}$. Finally, inte-

grating we get

$$f_{\alpha,\mu,\sigma}(\mathbf{z}) = \tfrac{2}{\alpha}\sqrt{\alpha\mathbf{z} - \alpha\mu + \sigma^2}. \tag{6}$$

The $3/8$ factor in the GAT accounts for additional terms in the variance expression [6].

Let $\mathbf{v}$ be an image generated according to Eq. (1) and set $\mu = 0$. Assume that (i) the variance-stabilizing transform constructed using the correct noise parameters achieves exact stabilization, i.e., $\mathrm{var}[f_{\alpha,\sigma}(\mathbf{v}) \,|\, \mathbf{u}] = 1$; (ii) for estimates $\hat{\alpha}, \hat{\sigma}$,

$$\mathrm{var}[f_{\hat{\alpha},\hat{\sigma}}(\mathbf{v}) \,|\, \mathbf{u}] = \left(f'_{\hat{\alpha},\hat{\sigma}}(\mathbf{z})\right)^2 \mathrm{var}[\mathbf{v} \,|\, \mathbf{u}]. \tag{7}$$

Proposition 1 ([9]) *We consider an image block B, with $p_B(\mathbf{u})$ being the PDF of $\mathbf{u}$ over B. The solution of*

$$\int \mathrm{var}[f_{\hat{\alpha},\hat{\sigma}}(\mathbf{v}) \,|\, \mathbf{u}]\, p_B(\mathbf{u})\, d\mathbf{u} = 1, \tag{8}$$

is locally a simple smooth curve in a neighborhood of (α, σ) in the $(\hat{\alpha}, \hat{\sigma})$ plane.

Proposition 1 yields an important algorithmic insight. As each image block generates a smooth curve in the $(\hat{\alpha}, \hat{\sigma})$ plane, when working with multiple blocks, the correct parameters should lie at the intersection of all these curves.

Makitalo and Foi [9] propose to estimate the noise parameters with the following two-step algorithm: (i) choose K patches $\mathbf{v}_k$ at random from image $\mathbf{v}$; (ii) compute the estimates $\hat{\alpha}, \hat{\sigma}$ using

$$\min_{\alpha,\sigma} \sum_{k=1}^{K} \ell(\mathrm{var}[f_{\alpha,\sigma}(\mathbf{v}_k) \,|\, \mathbf{u}_k] - 1), \tag{9}$$

where ℓ is a non-linearity (e.g., the Huber loss). This is a highly non-convex optimization problem and solving it in practice is not easy [9]. Other alternatives also propose fairly complicated algorithmic chains [10].

The HT is a natural candidate to solve this estimation problem (i.e., find the intersection of curves on a plane). First, the parameter space is low-dimensional. Second, we know in advance that we are interested in detecting a single GAT (a single parametric model), which significantly simplifies the use of the HT. Finally, it is fully parallelizable, which is a significant advantage for video processing.

2.1. Specifying the Hough transform

The input dataset is composed of K 2D patches $\{\mathbf{v}_k\}_{k=1}^K$ extracted from the noisy image $\mathbf{v}$. In videos, we just extract 2D patches from different frames to avoid dealing with motion. By default, we use 8×8 patches.

Using the GAT (Eq. (4)) as our variance stabilization method of choice implies that the cases $\mathbf{n}(\mathbf{x}) \sim \mathcal{N}(\mu, \sigma^2)$ and $\mathbf{n}(\mathbf{x}) \sim \mathcal{N}(0, \sigma^2 - \alpha\mu)$ are treated indistinctly. We will thus generically set $\beta = \sigma^2 - \alpha\mu$, implying that $\mathbf{n}(\mathbf{x}) \sim \mathcal{N}(0, \beta)$. Then, our simplified GAT is

$$f_{\alpha,\beta}(\mathbf{z}) = 2\sqrt{\max\left(\tfrac{\mathbf{z}}{\alpha} + \tfrac{3}{8} + \tfrac{\beta}{\alpha^2}, 0\right)}. \tag{10}$$

Notice that this change of variables reduces the parameter space from the original three dimensions to just two (μ cannot be disentangled from $\alpha\mathbf{u}$ anyway).

With our target $\mathrm{var}[f_{\alpha,\beta}(\mathbf{v}) \,|\, \mathbf{u}] = 1$ in sight, we define our parametric model as the zeroth iso-level of a function

$$h(\alpha, \beta) = \{\mathbf{u}_*\,,\ \mathrm{var}[f_{\alpha,\beta}(\mathbf{v}_*) \,|\, \mathbf{u}_*] - 1\}, \tag{11}$$

where $\mathbf{u}_*$ is a patch not necessarily contained in our dataset.

The HT uses a 2D array A, called an accumulator, which is a discretized version of the plane defined by α and β. Each bin (i, j) in the accumulator encodes a pair (α_i, β_j). Unfortunately, it is not trivial to discretize this space, as no upper and lower bounds are known a priori. Let us explain how we build and populate the accumulator, as detailed in Alg. 1.

From eqs. (2a) and (2b), we get the relation

$$\mathrm{var}[\mathbf{v} \,|\, \mathbf{u}] = \alpha\, \mathrm{E}[\mathbf{v} \,|\, \mathbf{u}] + (\sigma^2 - \alpha\mu) = \alpha\, \mathrm{E}[\mathbf{v} \,|\, \mathbf{u}] + \beta, \tag{12}$$

and the linear system [11, 12],

$$(\forall k)\ \mathrm{var}[\mathbf{v}_k \,|\, \mathbf{u}_k] = \alpha\, \mathrm{E}[\mathbf{v}_k \,|\, \mathbf{u}_k] + \beta. \tag{13}$$

Using robust linear regression (with a Huber loss), we obtain the initial estimates α_{init} and β_{init}. These estimates constitute the center bin of our accumulator. We then build suitable (conservatively large) ranges for α and β and discretized values for α_i and β_j. We are interested in patches that lie very

Alg. 1: Noise estimation with the Hough transform

input : noisy image $\mathbf{v}$, number K of patches to use.
output : GAT parameter estimates α_{final}, β_{final}.

Choose the random patches $\{\mathbf{v}_k\}_{k=1}^K$ from $\mathbf{v}$;
Solve the linear system in Eq. (13) obtaining α_{init}, β_{init};
$\Delta_\alpha \leftarrow 0.9\alpha$;
$\Delta_\beta \leftarrow \max(2 \cdot 10^3, |\beta_{\text{init}}|)$;
`// Build coarse accumulator space`
Get 100 equally spaced samples α_i in the interval $[\alpha_{\text{init}} - \Delta_\alpha, \alpha_{\text{init}} + \Delta_\alpha]$;
Get 100 equally spaced samples β_j in the interval $[\beta_{\text{init}} - \Delta_\beta, \beta_{\text{init}} + \Delta_\beta]$;
$(\forall i, j)\ A^{\text{coarse}}_{i,j} \leftarrow \sum_{k=1}^K \mathrm{SM}(\mathrm{var}[f_{\alpha_i,\beta_j}(\mathbf{v}_k) \,|\, \mathbf{u}_k] - 1)$
$\alpha_{\text{mid}}, \beta_{\text{mid}} \leftarrow \mathrm{argmax}_{i,j}\, A^{\text{coarse}}_{i,j}$;
`// Build focused accumulator space`
Get 100 equally spaced samples α_i in the interval $[\alpha_{\text{mid}} - \Delta_\alpha/4, \alpha_{\text{mid}} + \Delta_\alpha/4]$;
Get 100 equally spaced samples β_j in the interval $[\beta_{\text{mid}} - \Delta_\beta/10, \beta_{\text{mid}} + \Delta_\beta/10]$;
$(\forall i, j)\ A^{\text{focus}}_{i,j} \leftarrow \sum_{k=1}^K \mathrm{SM}(\mathrm{var}[f_{\alpha_i,\beta_j}(\mathbf{v}_k) \,|\, \mathbf{u}_k] - 1)$
$\alpha_{\text{final}}, \beta_{\text{final}} \leftarrow \mathrm{argmax}_{i,j}\, A^{\text{focus}}_{i,j}$;

Table 1. Incorporating variance stabilization as a pre-processing improves the performance of neuron detection in calcium imaging data using an online NMF-based algorithm [15]. Performance is quantified using precision, recall and the F_1 score (their harmonic mean).

	VST+OnACID	OnACID
F_1 score	**0.82**	0.80
Precision	**0.83**	0.78
Recall	0.81	**0.82**

close to our parametric model. We populate the accumulator using the formula

$$A_{i,j} = \sum_{k=1}^{K} \mathrm{SM}(h(\alpha_i, \beta_j)), \tag{14}$$

where h is defined in Eq. (11) and $\mathrm{SM}(s) = \exp(-(s/\epsilon)^2))$ and $\epsilon = 10^{-2}$. This soft-membership function allows to account for small inaccuracies in the estimation.

Noticing that the populated accumulator is in general relatively smooth, we use two scales to accelerate the algorithm's running time. We first build a coarse accumulator and detect its peak. Zooming in an small area around the peak, we build a finer accumulator and populate it using Eq. (14). The peak of this focused accumulator constitutes our final estimation.

A missing ingredient in Alg. 1 is the computation of $\mathrm{E}[\mathbf{w}_k \,|\, \mathbf{u}_k]$ and $\mathrm{var}[\mathbf{w}_k \,|\, \mathbf{u}_k]$ without knowing $\mathbf{u}_k$ ($\mathbf{w}_k = \mathbf{v}_k$ in Eq. (12) or $\mathbf{w}_k = f_{\alpha,\sigma}(\mathbf{v}_k)$ in Eq. (14)). Depending on the amount of structure (texture, edges, etc.) in the patches, different estimators can be employed: from sample mean and variance [12], to high-pass filters [9, 13], to more sophisticated methods [14]. In our experiments with calcium imaging, we use the sample mean and variance for simplicity.

Finally, several constants are used for the creation of the accumulators in Alg. 1. These should provide ample ranges for α and β and their details are application-specific (we detail our choices for calcium imaging data).

3. APPLICATION TO CALCIUM IMAGING DATA

We tested the utility of the GAT, with parameters estimated using the proposed method, as a pre-processing step for detecting neurons in two photon fluorescent microscopy time series data (calcium imaging) [16]. In general, the spatio-temporal activity of each neuron is expressed by the outer product of a vector in space that expresses the location and shape of each neuron, and a vector in time that expresses its activity during the experiment. Then the neurons can be extracted using matrix factorization methods, such as independent components analysis [17] or non-negative matrix factorization [18, 19].

While effective, these approaches typically rely on Gaussian noise assumptions, an assumption that is violated by the multiplicative characteristics of the microscope photon

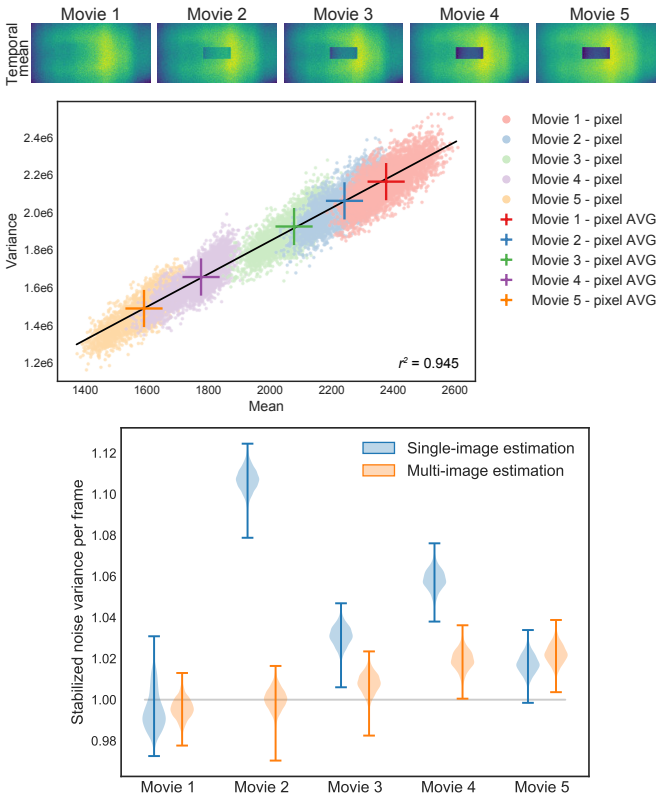

Fig. 1. Testing the Poisson-Gaussian as measurement noise model for 2p imaging data using fluorescent beads. **Top:** Mean across time of the fluorescence over the entire FOV. A part in the center of the FOV is progressively ablated to expose different mean fluorescence levels. **Middle:** Variance versus mean plot for all pixels and all movies. A linear fit explains the observed scatter plot ($r^2 = 0.945$), justifying the Poisson-Gaussian noise model. **Bottom:** Histograms of each frame's variance after the VST application. The VST equalizes the variance (the target is 1), and performs better when estimated over multiple frames (10 in this case).

noise. We first tested whether measurement noise in calcium imaging can be described by the Poisson-Gaussian model (a model that has been used in other studies, e.g., [7]), by gathering noise statistics on synthetic fluorescent beads that were progressively photobleached around the center to expose five different levels of fluorescence emissions (Fig. 1-top). For individual pixels, the variance scales linearly with the mean ($r^2 = 0.945$) across all different movies (Fig. 1-middle). When dealing with the mean and variance of 8×8 patches, the results were largely the same (data not shown). We then applied the Hough-VST transform, as estimated from a single or multiple ($N = 10$) frames for each movie. Fig. 1-bottom shows histograms of the variance of individual pixels for all different movies, and demonstrates that the transformation stabilizes the variance across the FOV when its parameters are estimated from multiple frames.

To test whether preprocessing the data by applying the GAT improves the performance of source extraction we use OnACID [15], a state of the art online NMF-based source extraction algorithm, on a 90000 frame long 500 μm $\times$ 500μm

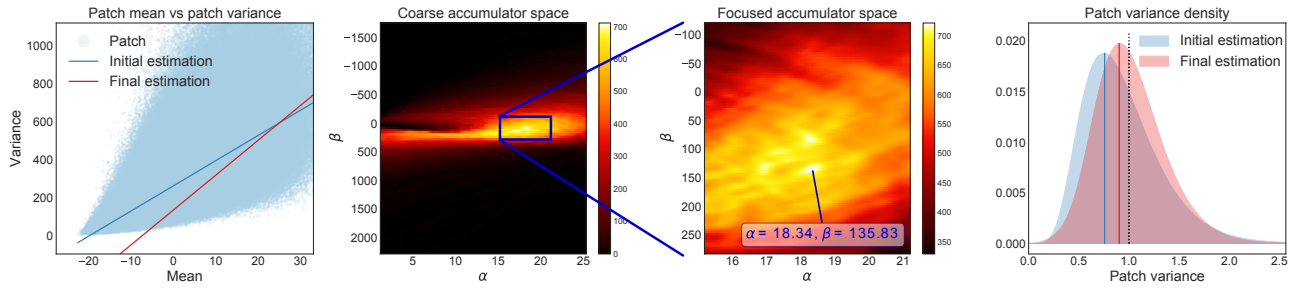

Fig. 2. Demonstration of the proposed Hough-based noise estimation pipeline. **Left:** Mean versus the variance scatter plot for every patch extracted from the video. The estimated parameters α, β are also plotted as lines, see Eq. (12). **Center left:** The coarse accumulator from Alg. 1. This accumulator looks like the typical Hough accumulator. **Center right:** The focused accumulator from Alg. 1. The detected peak might not be at its very center. No new spurious peaks appear when zooming-in in the desired area, making the proposed two-scale approach fast and accurate. **Right:** We compute the sample variance of every patch after applying the GAT using the initial and the final estimates. Alg. 1 further stabilizes the variance (bringing it closer to 1).

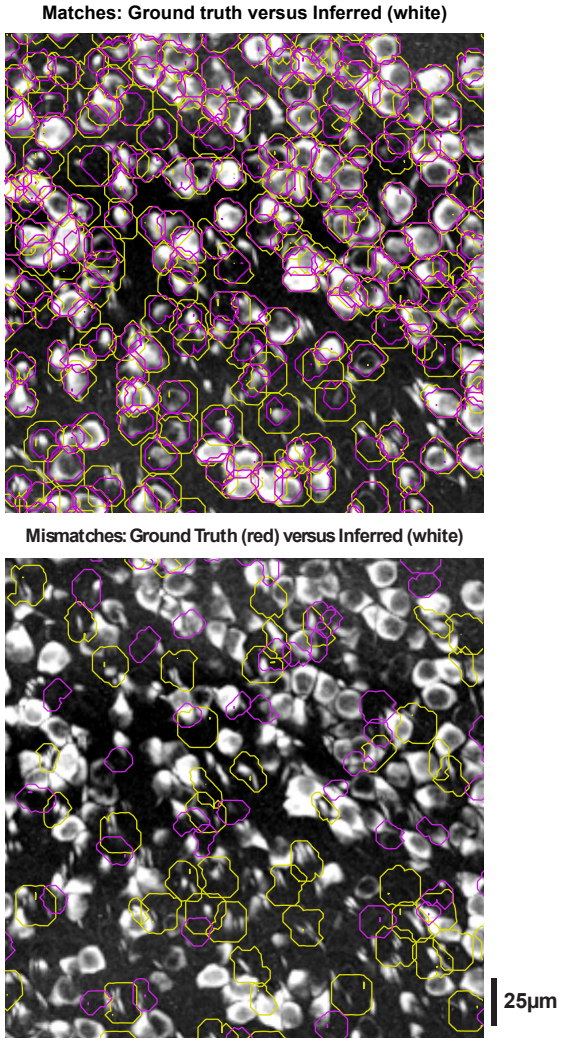

Fig. 3. Preprocessing calcium imaging data with the GAT enhances the performance of source detection algorithms. **Left:** Matches between inferred (white) and manually annotated (red) ROIs on an *in vivo* mouse hippocampus dataset. **Right:** False positive (white) and false negative (red) mismatches between ground truth and inferred ROIs. All contour plots are superimposed on the correlation image of the dataset. For ease of exposition only a 250μm $\times$ 250μm part of the FOV is displayed in the figure.

large field of view *in vivo* mouse hippocampus dataset, imaged at 30Hz using the GCaMP3 indicator [20]. Fig. 2 details the process of the estimating the noise parameters according to Alg. 1 and the stabilization effect of applying the resulting GAT. We then used OnACID on the stabilized data to perform source extraction. Performance was quantified by detecting the locations of active neurons in the FOV when compared to manual annotations, measuring precision/recall with an intersection over union metric (see [15] for more details). The results (Tab. 1) indicate that applying the GAT improves the performance of OnACID in terms of the F_1 score, and enables the accurate detection of most neurons in the FOV (Fig. 3). These preliminary results indicate that the GAT transform is a simple tool that can be incorporated, along with the proposed parameter estimation method, in the calcium imaging data analysis pipelines and improve their performance.

4. CONCLUSIONS

We posed the parameter estimation of the Poisson-Gaussian noise model as a parametric model estimation problem. We first take patches from the image/video to analyze and treat the Generalized Anscombe transform as a parametric model, which we fit to the patches using the Hough transform. This simple estimation algorithm is able to successfully estimate the noise parameters, is computationally efficient, and is fully parallelizable. We additionally presented an application to calcium imaging data, where the estimated parameters were used to enhance state-of-the-art processing pipelines.

As future work, we will further explore the use of variance stabilization in calcium imaging. We are also aware that there are many modern techniques for parametric model estimation, and will consider their us in our particular case.

Acknowledgements. We thank L. Russell and M. Hausser (UCL) for performing the fluorescent bead imaging measurements. We thank J. Gauthier and D. Tank (Princeton University) for sharing the mouse hippocampus data. We thank B. Cohen, L. Myers, N. Roumelioti, and S. Villani for performing manual annotations of the imaging datasets.

5. REFERENCES

[1] Jean-Luc Starck, Fionn D Murtagh, and Albert Bijaoui, "Image Processing and Data Analysis," *Image Processing and Data Analysis*, 1998. 1

[2] Cédric Vonesch, François Aguet, Jean Luc Vonesch, and Michael Unser, "The colored revolution of bioimaging," *IEEE Signal Processing Magazine*, vol. 23, no. 3, pp. 20–31, 2006. 1

[3] A. Buades, B. Coll, and J. M. Morel, "A Review of Image Denoising Algorithms, with a New One," *Multiscale Modeling & Simulation*, vol. 4, no. 2, pp. 490–530, 2005. 1

[4] Kostadin Dabov and Alessandro Foi, "Image Denoising with Block-matching and {3D} Filtering," *Electronic Imaging*, vol. 6064, pp. 1–12, 2006. 1

[5] Pierrick Coupé, Martin Munz, Jose V. Manjón, Edward S. Ruthazer, and D. Louis Collins, "A CANDLE for a deeper in vivo insight," *Medical Image Analysis*, vol. 16, no. 4, pp. 849–864, 2012. 1

[6] Francis J Anscombe, "The transformation of Poisson, binomial and negative-binomial data," *Biometrika*, vol. 35, no. 3/4, pp. 246–254, 1948. 1, 2

[7] Cezar M Tigaret, Krasimira Tsaneva-Atanasova, Graham L Collingridge, and Jack R Mellor, "Wavelet transform-based de-noising for two-photon imaging of synaptic ca 2+ transients," *Biophysical journal*, vol. 104, no. 5, pp. 1006–1017, 2013. 1, 3

[8] Richard O. Duda and Peter E. Hart, "Use of the Hough transformation to detect lines and curves in pictures," *Communications of the ACM*, vol. 15, no. 1, pp. 11–15, 1972. 1

[9] Markku Makitalo and Alessandro Foi, "Noise Parameter Mismatch in Variance Stabilization, with an Application to Poisson-Gaussian Noise Estimation," *IEEE Transactions on Image Processing*, vol. 23, no. 12, pp. 5348–5359, 2014. 2, 3

[10] Stanislav Pyatykh and Jurgen Hesser, "Image Sensor Noise Parameter Estimation by Variance Stabilization and Normality Assessment," *IEEE Transactions on Image Processing*, vol. 23, no. 9, pp. 3990–3998, 2014. 2

[11] Jérôme Boulanger, *Jérôme Boulanger Estimation non-paramétrique et contributions à l ' analyse de séquences d ' images Modélisation , simulation et estimation du trafic intra-cellulaire dans des séquences de vidéo-microscopie .*, Ph.D. thesis, Université de Rennes I, 2007. 2

[12] Florian Luisier, *The SURE-LET approach to image denoising*, Ph.D. thesis, EPFL, 2010. 2, 3

[13] Miguel Colom and Antoni Buades, "Analysis and Extension of the Percentile Method, Estimating a Noise Curve from a Single Image," *Image Processing On Line*, vol. 3, pp. 332–359, 2013. 3

[14] Miguel Colom and Antoni Buades, "Analysis and Extension of the Ponomarenko et al. Method, Estimating a Noise Curve from a Single Image," *Image Processing On Line*, vol. 3, pp. 173–197, 2013. 3

[15] Andrea Giovannucci, Johannes Friedrich, Johannes Kaufman, Anne Churchland, Dmitri Chklovskii, Liam Paninski, and Eftychios A. Pnevmatikakis, "OnACID: Online analysis of calcium imaging data in real time," in *Neural Information Processing Systems (NIPS)*, 2017. 3, 4

[16] Lin Tian, S Andrew Hires, Tianyi Mao, Daniel Huber, M Eugenia Chiappe, Sreekanth H Chalasani, Leopoldo Petreanu, Jasper Akerboom, Sean A McKinney, Eric R Schreiter, Cornelia I Bargmann, Vivek Jayaraman, Karel Svoboda, and Loren L Looger, "Imaging neural activity in worms, flies and mice with improved GCaMP calcium indicators," *Nature Methods*, vol. 6, no. 12, pp. 875–881, dec 2009. 3

[17] Eran A Mukamel, Axel Nimmerjahn, and Mark J Schnitzer, "Automated analysis of cellular signals from large-scale calcium imaging data," *Neuron*, vol. 63, no. 6, pp. 747–760, 2009. 3

[18] Ryuichi Maruyama, Kazuma Maeda, Hajime Moroda, Ichiro Kato, Masashi Inoue, Hiroyoshi Miyakawa, and Toru Aonishi, "Detecting cells using non-negative matrix factorization on calcium imaging data," *Neural Networks*, vol. 55, pp. 11–19, 2014. 3

[19] Eftychios A Pnevmatikakis, Daniel Soudry, Yuanjun Gao, Timothy A Machado, Josh Merel, David Pfau, Thomas Reardon, Yu Mu, Clay Lacefield, Weijian Yang, et al., "Simultaneous denoising, deconvolution, and demixing of calcium imaging data," *Neuron*, vol. 89, no. 2, pp. 285–299, 2016. 3

[20] J. Gauthier and D.W. Tank, "A subset of ca1 and subiculum neurons selectively encode rewarded locations," in *Computational and Systems Neuroscience Meeting, Cosyne*, 2016. 4